

Published in final edited form as:

*Biochemistry*. 2011 October 4; 50(39): 8374–8382. doi:10.1021/bi2009079.

## Mechanism of Ribonuclease A Endocytosis: Analogies to Cell-Penetrating Peptides†

Tzu-Yuan Chao<sup>‡,§</sup> and Ronald T. Raines<sup>‡,||,\*</sup>

<sup>‡</sup>Department of Biochemistry, University of Wisconsin–Madison, Madison, Wisconsin 53706, United States

<sup>||</sup>Department of Chemistry, University of Wisconsin–Madison, Madison, Wisconsin 53706, United States

### Abstract

Pancreatic-type ribonucleases can exert toxic activity by catalyzing the degradation of cellular RNA. Their ability to enter cells is essential for their cytotoxicity. Here, we determine the mechanism by which bovine pancreatic ribonuclease (RNase A) enters human cells. Inhibiting clathrin-dependent endocytosis with dynasore or chlorpromazine decreases RNase A-uptake by ~70%. Limited colocalization between RNase A and transferrin indicates that RNase A is not routed through recycling endosomes. Instead, vesicular staining of RNase A overlaps substantially with that of nonaarginine and the cationic peptide corresponding to residues 47–57 of the HIV-1 TAT protein. At low concentrations (<5 μM), internalization of RNase A and these cell-penetrating peptides (CPPs) is inhibited by chlorpromazine as well as the macropinocytosis inhibitors cytochalasin D and 5-(*N*-ethyl-*N*-isopropyl)amiloride to a similar extent, indicative of common endocytic mechanism. At high concentrations, CPPs adopt a non-endocytic mechanism of cellular entry that is not shared by RNase A. Collectively, these data suggest that RNase A is internalized via a multi-pathway mechanism that involves both clathrin-coated vesicles and macropinosomes. The parallel between the uptake of RNase A and CPPs validates reference to RNase A as a “cell-penetrating protein”.

### Keywords

cell-penetrating peptide; clathrin-coated vesicles; cytotoxin; endocytosis; macropinocytosis; onconase

The pancreatic-type ribonuclease family encompasses a large group of secretory enzymes with diverse biological actions, including neovascularization activity by angiogenin (1, 2), bactericidal and antiviral activities by the eosinophil cationic protein (ECP) (3, 4), and cytotoxic activity by ECP, bovine-seminal ribonuclease, Onconase<sup>®</sup> (ONC), and variants of bovine pancreatic ribonuclease (RNase A) and human pancreatic ribonuclease (5–7). Internalization by the target cell is an indispensable step in this broad range of activities (8, 9). ONC and an RNase 1 variant demonstrate selective toxicity towards cancer cells and are in human clinical trials as chemotherapeutic agents. Still, little is known about the mechanism of cellular uptake of these ribonucleases.

<sup>†</sup>This work was supported by Grant R01 CA073808 (NIH). T.-Y.C. was supported by the Dr. James Chieh-Hsia Mao Wisconsin Distinguished Graduate Fellowship.

\*Address correspondence to this author. Telephone: 608-262-8588. Fax: 608-890-2583. rtraines@wisc.edu.

<sup>§</sup>Current address: Novo Nordisk China, No. 29 Life Science Park Road, Changping District, Beijing 102206, China.

Mammalian cells have an intricate endocytic system with several parallel pathways. Of these pathways, one of the best characterized is clathrin-mediated endocytosis, which occurs constitutively in all mammalian cells (10). Receptor · ligand complexes destined for clathrin-mediated endocytosis are recruited by adaptor protein complex AP2 to clathrin-coated pits (11). In the final step of endocytosis, the GTPase dynamin is required for fission of the clathrin-coated vesicles (11). Transferrin is a widely recognized marker of clathrin-mediated endocytosis (10). Another well-characterized endocytic pathway is caveolar-mediated endocytosis. Similar to clathrin-mediated endocytosis, the coat protein caveolin-1 is necessary for the formation of caveolae; dynamin is also implicated in this pathway (12). Caveolar-dependent uptake has been associated with cholesterol- and sphingolipid-rich plasma microdomains known as lipid rafts, though the raft domains could also be internalized through non-caveolar pathways, such as macropinocytosis (13). The formation of macropinosomes often involves membrane ruffling, an actin-dependent process, but does not require dynamin (14). Molecules known to use this route for cellular entry include dextran, horseradish peroxidase, and the cell-penetrating peptides (CPPs) polyarginine and residues 47–57 of the HIV-1 trans-activator of transcription (TAT) (14–16). Finally, there are additional clathrin- and caveolar-independent endocytic pathways that are less characterized and often defined only by specific markers (17).

Clathrin-mediated pathways rely on specific cell-surface receptors. Although colocalization with transferrin implicates a clathrin-dependent mechanism for ONC uptake (18), the existence of specific receptors for ONC on mammalian cell surfaces is debatable. Two saturable binding sites with  $K_d$  values of 0.062 and 0.25  $\mu\text{M}$  were proposed to exist on 9L glioma cells (19), though the binding of ONC to HeLa cells was later shown to be non-saturable at protein concentrations up to 10  $\mu\text{M}$ , indicative of nonspecific binding (20). Consistent with the latter result, cationic residues in pancreatic-type ribonucleases have been proposed to participate in nonspecific Coulombic interactions with anionic cell-surface moieties (21–23).

ECP, which is the most cationic pancreatic-type ribonuclease, has been shown to interact with anionic cell-surface heparan sulfate proteoglycans (HSPGs) (24). A thorough characterization of HSPG-mediated ECP-uptake revealed independence of both clathrin and caveolin. Moreover, a requirement for actin, phosphoinositide-3-kinase (PI3K), ADP-ribosylation factor 6, and Ras-related botulinum toxin substrate 1 showed unambiguously that ECP was taken up into Beas-2B human bronchial epithelial cells by raft-dependent macropinocytosis (24).

RNase A has also been shown to interact with cell-surface HSPGs, which mediate its uptake (25). In accord with this finding, the cytotoxicity of a variant of RNase A was unaffected by the overproduction of K44Adynamin, indicative of a dynamin-independent mechanism (20). Other aspects of the uptake mechanism are, however, less clear.

Here, we delineate the pathway(s) by which RNase A enters live human cells. To do so, we make use of small-molecule fluorescent tags that enable the detection of cellular entry and small-molecule pharmacological agents that inhibit specific endocytic pathways. By comparing the uptake and subsequent cellular distribution of RNase A with those of nonaarginine ( $R_9$ ) and TAT, we conclude that RNase A is an exemplary “cell-penetrating protein”.

## EXPERIMENTAL PROCEDURES

### Materials

*Escherichia coli* strain BL21 (DE3) and plasmid pET22b(+) were from Novagen (Madison, WI). Endocytic inhibitors *Zygosporium mansonii* cytochalasin D (CD), chlorpromazine hydrochloride, 5-(*N*-ethyl-*N*-isopropyl)amiloride (EIPA), dynasore, *Penicillium funiculosum* wortmannin, nystatin, and methyl- $\beta$ -cyclodextrin (M $\beta$ CD) were from Sigma-Aldrich (St. Louis, MO). Endocytic markers Alexa Fluor 594-transferrin and Alexa Fluor 594-cholera toxin B subunit were from Invitrogen (Carlsbad, CA). Tetramethylrhodamine-labeled dextran (MW 65-76K) was from Sigma-Aldrich. FAM-TAT, TAMRA-TAT, FAM-R<sub>9</sub>, and TAMRA-R<sub>9</sub>, which are labeled on their N-termini, were from Anaspec (Fremont, CA). All other chemicals and reagents were of commercial reagent grade or better, and were used without further purification.

### Mammalian Cell Culture

HeLa cells were from the American Type Culture Collection (Manassas, VA) and grown in minimum essential medium containing fetal bovine serum (10% v/v), penicillin (100 units/mL), and streptomycin (100  $\mu$ g/mL). Cell culture medium and supplements were from ATCC. Cells were cultured at 37 °C in a humidified incubator containing CO<sub>2</sub>(g) (5% v/v).

### Instrumentation

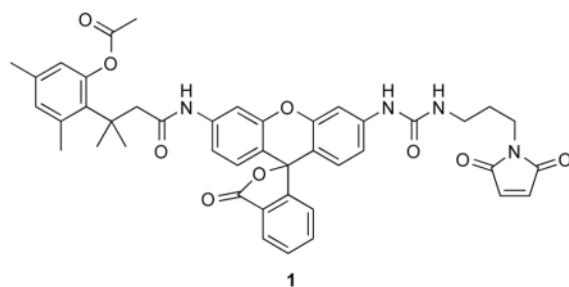
Molecular mass was measured by MALDI-TOF mass spectroscopy using a Voyager-DE-PRO Biospectrometry Workstation (Applied Biosystems, Foster City, CA) with sinapinic acid as a matrix in the campus Biophysics Instrumentation Facility. Flow cytometry data were collected in the University of Wisconsin Paul P. Carbone Comprehensive Cancer Center with a FACS Calibur flow cytometer equipped with a 488-nm argon-ion laser (Becton Dickinson, Franklin Lakes, NJ). Microscopy images were obtained with a Nikon C1 laser scanning confocal microscope with a 60 $\times$  oil immersion objective with NA 1.4.

### Production and Purification of Ribonucleases

Wild-type RNase A and its A19C variant were produced in *E. coli* BL21(DE3) cells and purified as described previously (26). Following purification, protein solutions were dialyzed against PBS and passed through a 0.2- $\mu$ m filter prior to use.

### Fluorescent Labeling of Ribonucleases

A19C RNase A contains a free cysteine residue for site-specific conjugation by *S*-alkylation (20). During its purification, the thiol group of Cys19 was protected by reaction with 5,5'-dithio-bis(2-nitrobenzoic acid). Immediately prior to fluorophore attachment, protected A19C RNase A was deprotected by treatment with a 4-fold excess of dithiothreitol, and the reaction mixture desalted by chromatography on a PD-10 desalting column (GE Biosciences, Piscataway, NJ). Deprotected A19C RNase A was reacted for 6 h at 25 °C with a 10-fold molar excess of either fluorescein-5-maleimide (Anaspec, Fremont, CA) or a maleimide-containing rhodamine<sub>110</sub>-based fluorogenic label, **1** (27). This label is not fluorescent until activated by intracellular esterases, such as those in endosomes, and thus enhances the clarity of endocytic entry. The resulting RNase A conjugates were purified by chromatography using a HiTrap SP HP column (GE Biosciences). The molecular masses of RNase A, its A19C variant, and its conjugates were confirmed by MALDI-TOF mass spectrometry. Protein concentration was determined by using a bicinchoninic acid assay kit (Pierce, Rockford, IL) with wild-type RNase A as a standard.



## Flow Cytometry

The internalization of RNase A conjugates was monitored directly in living cells. HeLa cells from near confluent flasks were plated in 6-well plates at  $1.2 \times 10^5$  cells/mL/well 18–24 h prior to experiments. Labeled proteins and peptides were added to each well, which were incubated at 37 °C for varying times. To quench internalization, cells were washed twice with ice-cold PBS, and treated with trypsin/EDTA for several minutes. Complete medium containing fetal bovine serum (10% v/v) was added to each well. Samples remained on ice until analyzed by flow cytometry. For drug sensitivity studies, cells were pretreated with drugs for 30 min in minimum essential medium (Invitrogen) followed by incubation with protein or peptide conjugates for 1 h at 37 °C.

Fluorescence was detected through a 530/30-nm band-pass filter. Cell viability was determined by staining with propidium iodide, which was detected with a 660-nm long-pass filter. The mean channel fluorescence intensity of 20,000 viable cells was determined for each sample using CellQuest software and used for subsequent analyses.

## Microscopy

HeLa cells were plated on Nunc Lab-tek II 8-well chambered coverglass (Fisher Scientific, Pittsburgh, PA) and grown to 70% confluency. Cells were then incubated with labeled conjugates for 1 h at 37 °C. Cell nuclei were stained by the addition of Hoechst 33342 (2 µg/mL) for the final 5 min of incubation. For pharmacological studies, cells were pretreated with compounds in minimum essential medium for 30 min at 37 °C.

Cells were imaged on a Nikon Eclipse TE2000-U laser scanning confocal microscope equipped with a Zeiss AxioCam digital camera. Excitation at 408 nm was provided by a blue-diode laser, and emission at 450 nm was passed through a 35-nm band-pass filter. Excitation at 488 nm was provided by an argon-ion laser, and emission at 515 nm was passed through a 40-nm band-pass filter. Excitation at 543 nm was provided by a HeNe laser, and emission at 605 nm was passed through a 75-nm band-pass filter.

## RESULTS

### Effect of Endocytic Inhibitors on RNase A-Uptake

Endocytic pathways can be distinguished by blocking specific molecular components with pharmacological agents. To determine the mechanism of cellular entry by RNase A, we examined RNase A-uptake in the presence of endocytic inhibitors qualitatively by using confocal microscopy and quantitatively by using flow cytometry. Specifically, we used dynasore (80 µM) to test for dependence on dynamin; chlorpromazine (CPZ; 10 µg/mL) and nystatin (25 µg/mL) as inhibitors of clathrin- and caveolar-mediated pathways, respectively; and CD (5 µg/mL) and EIPA (10 µM) as probes for macropinocytosis. We also used MβCD (5 mM) and wortmannin (50 nM) to assess the requirement for cholesterol and PI3K, respectively, during RNase A internalization. The use of each of these inhibitory compounds

in mammalian cell lines is well-established (28, 29). Here, pretreatments with a drug for 30 min at 37 °C resulted in expected effects on the uptake of the endocytic markers transferrin, cholera toxin subunit B (CTB), and dextran (data not shown). Toxicity did not exceed 5% of the cell population during the course of an experiment.

The dominant-negative K44A dynamin variant has been used widely to probe the internalization of various molecules (30), including RNase A (20). Still, tetracyclin-induced overexpression of K44A dynamin in HeLa cells has been reported to lead to an increase in endosomal pH by 0.4–0.7 units (18, 31). This change in pH might not affect early endocytic events, but could alter the trafficking of internalized molecules. For example, a decrease in the IC<sub>50</sub> value of ONC upon K44A dynamin expression was suggested to be due to increased translocation as a result of a change in endosomal pH (18). As a similar decrease in IC<sub>50</sub> value was observed for RNase A in K44A dynamin cells, we sought to revisit the dynamin-dependence of RNase A-uptake by using dynasore, a noncompetitive inhibitor of the GTPase activity of dynamin (28). Dynasore abolishes dynamin activity within 30 min of incubation, thereby providing temporal control superior to that of tetracycline-induced expression of K44A dynamin. No obfuscating biological effects have been associated with dynasore treatment. Unexpectedly, the endocytosis of RNase A was highly sensitive to dynasore treatment; the level of internalization was reduced to a third (Figure 1B). The cellular distribution of RNase A was sparse and dispersed in dynasore-treated cells (Figure 1Aii). The marked decrease in internalization indicates that RNase A-uptake is dependent on dynamin, at least in part.

Both clathrin- and caveolar-mediated pathways require the action of dynamin in the process of vesicle scission (10). To determine which dynamin-dependent pathway is involved in RNase A-uptake, we treated cells with CPZ and nystatin. CPZ is an amphiphilic cationic drug known to disrupt clathrin-mediated endocytosis (32), as well as a pathway distinct from clathrin-mediated endocytosis that is characterized by the formation of cell-surface nucleation zones and is utilized by cell-penetrating peptides at high concentrations (33). Treatment with CPZ reduced RNase A internalization to a third without affecting its localization (Figures 1Aiii and 1B). In contrast, RNase A-uptake was decreased only slightly in the presence of nystatin (Figures 1Aiv and 1B), which is a selective inhibitor of the lipid raft/caveolae pathway (29). Cholesterol extraction with M $\beta$ CD also had little effect on RNase A-uptake (Figures 1Av and 1B). These results indicate that the internalization of RNase A is mediated by a CPZ-sensitive pathway, possibly involving clathrin, but not by a lipid raft/caveolae-dependent endocytic pathway.

Dynasore treatment did not abolish RNase A-uptake completely. Accordingly, we tested other inhibitors of macropinocytosis, a dynamin-independent pathway (34). CD is an F-actin depolymerizing drug that blocks membrane ruffling and hence macropinocytosis (35). Although formation of macropinosomes is most sensitive to CD treatment, CD is also believed to affect endocytosis via clathrin-coated pits and caveolae, which depend on actin to a lesser extent (36, 29). Here, we found that RNase A-uptake was reduced to a quarter (Figure 1Avi and 1B) in CD-treated cells; likewise, transferrin-uptake was reduced to two thirds (data not shown). The sensitivity to CD treatment suggests that the actin cytoskeleton is required for RNase A-uptake, but does not necessarily imply the involvement of macropinocytosis. Next, we tested the effects of EIPA, a selective inhibitor of the Na<sup>+</sup>/H<sup>+</sup> antiporter specific to macropinocytosis (37). Treatment with EIPA (Figure 1Avii) decreases peripheral RNase A-staining compared with non-treated cells (Figure 1Ai), and decreases RNase A-uptake to two thirds (Figure 1B). These results, together with those from CD treatment, indicate that macropinocytosis is partially responsible for mediating RNase A entry. Further, co-treatment with CD and either dynasore or CPZ resulted in a nearly



complete loss of RNase A-uptake by HeLa cells (Figure 1B), which is consistent with RNase A being internalized largely via macropinocytosis and clathrin-mediated pathways.

The fungal metabolite wortmannin inhibits the enzymatic activity of PI3K (38). Though it has been used to block constitutive and stimulated macropinocytosis in some cell types, the role of PI3K in macropinocytosis is not well-established (29). Wortmannin is also known to inhibit homotypic fusion of early endosomes (39). Indeed, RNase A-staining in wortmannin-treated cells was more dispersed and RNase A-containing vesicles were smaller in size (Figure 1Aviii). Yet, the overall level of internalization was unaffected by wortmannin (Figure 1B), suggesting that PI3K activity is not required for RNase A-uptake.

### RNase A Colocalizes with CTB and the CPPs

To analyze further the route of cellular entry by RNase A, we examined the colocalization of RNase A with various endocytic markers. RNase A (10  $\mu$ M) and transferrin (1  $\mu$ M) were incubated with wild-type HeLa cells for 1 h at 37 °C. Transferrin exhibits rapid uptake and labels early sorting endosomes and recycling compartments (11). RNase A-uptake is comparatively slower in HeLa cells. As a result, a 1-h incubation was allowed to facilitate visualization of its subcellular distribution. Limited overlap between transferrin and RNase A was apparent (Figure 2i). The majority of transferrin-positive vesicles appear to be smaller in size and distinct from RNase A-containing compartments. The two were found to colocalize in perinuclear compartments, which are likely the rab11-positive recycling endosomes in which transferrin resides (40). This finding is consistent with previous reports on RNase A-uptake, which demonstrated that RNase A does not colocalize with transferrin in K-562 cells and in K44A dynamin HeLa cells (20). Although sensitivity to CPZ and dynasore treatment is indicative of a clathrin-mediated mechanism for RNase A internalization, its localization suggests that the routing of RNase A is distinct from that of transferrin.

Next, we analyzed colocalization of RNase A and CTB. CTB prefers the caveolar-mediated pathway but can also be internalized by other pathways. In cells with low levels of caveolin-1 expression, such as HeLa cells, roughly 50% of CTB is internalized via clathrin-coated pits (41). Another pathway implicated in CTB-uptake involves clathrin-independent carriers (17, 34). They are typically tubular or ring-shaped endocytic structures whose formation does not require dynamin or coat proteins (34). Surprisingly, there was extensive colocalization between RNase A and CTB (Figure 2ii), both in peripheral endocytic vesicles and perinuclear compartments. As pathways dependent on clathrin or clathrin-independent carriers are the main routes by which CTB is taken up by HeLa cells, a high degree of colocalization is indicative of the involvement of both pathways in RNase A-uptake.

The cell-penetrating peptides constitute a class of short cationic polypeptides that enter cells efficiently. Owing to their small size and ability to deliver various molecules into mammalian cells, CPPs have potential value as vehicles in drug delivery (42). The internalization of CPPs has been studied thoroughly, but data concerning the mechanisms of uptake are not always consistent for the same peptides. For example, TAT was reported to be taken up by lipid raft-dependent macropinocytosis (15, 43) and clathrin-dependent endocytosis (44, 45) in HeLa cells. Moreover, a recent report showed that both R<sub>9</sub> and TAT utilize all three major endocytic pathways *simultaneously*, in addition to an apparently non-endocytic entry pathway (33).

To discern if RNase A shares a common endocytic route(s) with the CPPs, we searched for their colocalization. When equimolar quantities of the two were added to cells at the same time, RNase A-uptake was reduced greatly, presumably due to competition for cell-surface binding sites (data not shown). Both RNase A and the CPPs bind to anionic cell-surface

glycans such as heparan sulfate and chondroitin sulfate (25, 46, 44). R<sub>9</sub> has a higher affinity for the cell-surface than does RNase A, as R<sub>9</sub>-uptake was unaffected by excess RNase A (data not shown). To visualize RNase A localization in the presence of CPPs, cells were pre-incubated with RNase A for 15 min prior to the addition of R<sub>9</sub> and TAT. RNase A-staining overlaps significantly with R<sub>9</sub>-positive vesicles, even in cells with prominent cytosolic staining of R<sub>9</sub> (Figure 2iii). Similarly, TAT colocalizes with RNase A both in perinuclear compartments and peripheral endocytic structures (Figure 2iv). To ensure that the strong colocalization is not merely a result of merging endocytic pathways, experiments were repeated with shorter incubation times. Upon co-incubation for 15 min, fewer and smaller vesicles were observed, but the overall degree of colocalization was similar (data not shown).

### **RNase A-Uptake is Independent of Concentration**

Above threshold concentrations, R<sub>9</sub> and TAT adopt a novel mode of cellular entry that entails the formation of nucleation zones at the cell surface and results in diffuse cytosolic staining (33). This pathway is sensitive to heparinase, CPZ, and the protein kinase C inhibitor rottlerin, but not wortmannin (33). Interestingly, although vesicles are not detected, dynamin is required for this novel cell-penetration process (33). Because the uptake of RNase A exhibits a similar drug-sensitivity pattern as does this pathway, we sought to determine if RNase A uses this pathway at higher concentrations by assessing the concentration-dependence of RNase A-uptake and localization. First, RNase A was conjugated to fluorescein for direct comparison to fluorescein-labeled R<sub>9</sub> and TAT. The conjugates were then incubated with HeLa cells for 30 min at 37 °C and washed extensively with serum-free medium prior to imaging. Fluorescein has a pK<sub>a</sub> of 6.3 (47), and its fluorescence decreases upon protonation. At 10 μM, cellular staining from fluorescein-labeled RNase A (Figure 3Ai) is less than that from rhodamine<sub>110</sub>-labeled RNase A (Figures 1 and 2), suggesting that the majority of internalized RNase A resides in acidic endosomes at this concentration. The subcellular distribution of RNase A is unchanged at 20 μM (Figure 3Aiv). In contrast, both R<sub>9</sub> and TAT had substantially greater fluorescence, presumably due to strong cytosolic staining (Figures 3Av and 3Avi). Flow cytometry quantitation of RNase A- and CPP-uptake revealed that both TAT- and RNase A-uptake increased steadily with increasing concentration, whereas R<sub>9</sub>-uptake increased sharply above 20 μM. Moreover, R<sub>9</sub>- and TAT-uptake is much greater than that of RNase A. Together, these results suggest that RNase A does not use the novel non- endocytic pathway for cellular entry and that RNase A-uptake is concentration independent.

### **Mechanisms of RNase A- and CPP-Uptake are Similar at Low Concentrations**

The contribution of different endocytic pathways for RNase A and CPP internalization were compared in cells treated with CD-, CPZ-, or EIPA. First, CPP-uptake was reduced to 80–90% at 1 μM CPP and 30–40% at 10 μM CPP upon treatment with CD (Figure 4A). The molecular basis for the increased sensitivity to the higher concentration of CD is unclear, but could result from actin being required for the non-endocytic mechanism. RNase A-uptake, on the other hand, is more dependent on actin than is CPP internalization. Second, as expected, the sensitivity to CPZ was highly concentration-dependent for the CPPs (Figure 4B). At 1 μM, R<sub>9</sub>- and TAT-uptake were highly sensitive to CPZ-treatment; at 10 μM, however, CPP-uptake increased in the presence of CPZ. A similar trend in CPP-uptake was also observed with EIPA treatment (Figure 4C). These results suggest that CPZ-treatment augmented the use of the non-endocytic pathway by CPPs at high concentration, whereas RNase A-uptake was still dependent on clathrin-mediated endocytosis and macropinocytosis at the same concentrations. In conclusion, based on sensitivity to these drugs, RNase A-uptake was similar to R<sub>9</sub> and TAT at low concentrations (≤5 μM), suggesting that the

mechanisms mediating RNase A-uptake overlaps significantly with those mediating the cellular entry of R<sub>9</sub> and TAT at low concentrations (Table 1).

## DISCUSSION

RNase A is a cationic protein that enters cells without the need for any specific receptors (25). A thorough understanding of the mechanisms underlying RNase A internalization not only elicits interest from a biological perspective but also has implications for the development of ribonuclease-based chemotherapeutic agents. Here, through a pharmacological approach, we have shown that macropinocytosis and clathrin-mediated endocytosis are both responsible for mediating the cellular entry of RNase A (Figure 5).

The involvement of clathrin-mediated endocytosis in RNase A-uptake was unexpected from previous reports. The cytotoxicity of an RNase A variant had been found to increase in the presence of the dominant-negative K44A dynamin variant, suggesting that dynamin does not have a role in RNase A internalization (20). This finding can, however, be reconciled with a multi-pathway model for RNase A internalization. For example, RNase A that is internalized through different pathways could have different endosomal escape efficiencies. A slight upregulation of macropinocytosis in cells that overproduce K44A dynamin could lead to greater delivery of cytotoxic RNase A molecules into the cytosol.

In the present study, RNase A-uptake in dynasore-treated cells was reduced to a third of that in untreated cells (Figure 1B). Because dynasore-treatment diminishes transferrin internalization by >95% (28), this high level of residual RNase A-uptake indicates that RNase A also uses a dynamin-independent mechanism for cellular entry. Alternatively, dynasore could reduce unstimulated fluid-phase endocytosis by 50–60% (14, 28); fluid-phase endocytosis in the absence of serum or epidermal growth factor has been shown to be a dynamin-dependent process (14). Yet, considering the strong overlap between CTB and RNase A as well as partial colocalization between transferrin and RNase A (Figures 2i and 2ii), the dynamin-dependent mechanism involved in RNase A-uptake is likely to be clathrin- or caveolar-dependent endocytosis. Caveolae inhibitors nystatin and M $\beta$ CD had only a minimal effect on RNase A-uptake (Figure 1B), suggesting that caveolar-dependent endocytosis is not a major mechanism utilized by RNase A in HeLa cells. We note, though, that HeLa cells have relatively low levels of caveolin-1 (48), and the contribution of caveolar-dependent endocytosis to RNase A-uptake could be greater in other types of cells. Finally, two thirds of RNase A-uptake was determined to be CPZ-sensitive (Figure 1B), which is consistent with a partial dependence on clathrin.

ONC is an RNase A homologue that is also internalized via clathrin-mediated endocytosis (18). Routing through transferrin-associated early recycling endosomes is thought to be an effective pathway for ONC due to better translocation efficiencies near neutral pH. On the other hand, our data show that RNase A does not accumulate in early recycling endosomes but colocalizes with transferrin only at perinuclear late endosomal structures (Figure 2i). Although both ribonucleases utilize clathrin-dependent pathways, differential routing could account for the differential cytotoxicity of ONC and RNase A variants. For example, ONC is  $\geq$  10-fold more toxic than RNase A variants towards A549, NCI/ADR-RES, and CHO cells (25, 49). Traversing in recycling endosomes could be advantageous to ribonuclease-mediated cytotoxicity.

Clathrin-dependent pathways are mediated by receptors. Previous studies have demonstrated that RNase A interacts with cell-surface HSPGs and sialic acid-containing glycoproteins through Coulombic interactions (25). Interestingly, HSPGs are receptors for cationic serum proteins such as fibroblast growth factors (FGFs) and vascular endothelial growth factor



(VEGF) (50, 51). By interacting with heparan sulfate, these proteins induce dimerization of the receptors and subsequent internalization via macropinocytosis (FGF2) and clathrin-dependent endocytosis (VEGF) (52, 53). The RNase A–heparan sulfate interaction might trigger endocytosis. Alternatively, RNase A could be internalized passively along with receptor · ligand complexes. Similar to RNase A, R<sub>9</sub> and TAT both interact with cell-surface HSPGs (44, 46) (Table 1). Coincidentally, their cellular uptake has been described as adsorptive rather than receptor-mediated, and all major pathways are implicated in the internalization of CPPs (33, 54). Thus, interaction with cell-surface sulfated glycosaminoglycans seems to invoke a multi-pathway mechanism of endocytosis. Depending on the exact display of proteoglycans on different cell types, certain pathways could dominate the internalization of a cationic molecule.

Sensitivity to CD and EIPA indicates macropinocytosis unequivocally in RNase A-uptake (Figure 1B). Macropinocytosis is an F-actin driven process involving membrane ruffling and formation of lamellipodia (34). Although no specific receptor is required for this endocytic pathway, membrane-associated proteoglycans are thought to be important in the induction of F-actin organization and macropinocytosis (55). Indeed, both ECP and the CPPs R<sub>9</sub> and TAT have been shown to interact with cell-surface proteoglycans and then internalized by macropinocytosis (15, 24, 43). A high content of arginine residues seems to be essential in inducing this pathway, as ECP (which contains 19 arginine and 1 lysine residue), is the only RNase A homologue known to be internalized solely by macropinocytosis (24). ONC (12 lysine and 3 arginine residues) is internalized via clathrin-mediated endocytosis (18); whereas RNase A (10 lysine and 4 arginine residues; Figure 6), is internalized by both pathways (Figure 5). Although all three ribonucleases are cationic proteins of similar size and structure, the number of lysine and arginine residues, their ratio, and their distribution (23) could play a role in determining the endocytic route. Unlike other cell-penetrating proteins, such as the transcription factor BETA2/NeuroD (56) and the rattlesnake toxin crotamine (57), the cationic residues in RNase A are not confined to a short segment in its primary structure but coalesce in its tertiary structure (Figure 6).

RNase A homologues are rare in having cell-penetrating ability of demonstrable clinical utility. RNase A is internalized by a multi-pathway endocytic mechanism similar to that of the CPPs (Figure 5). In comparison to well-known determinants of ribonuclease-mediated cytotoxicity (49, 58, 59), the uptake of ribonucleases affords an opportunity for marked improvement (Figure 3). Hence, the findings reported herein inform the development of superior ribonuclease-based chemotherapeutic agents, as well as the creation of other useful cell-penetrating proteins (60, 61).

## Acknowledgments

We are grateful to L. D. Lavis (Janelia Farm Research Campus, Howard Hughes Medical Institute) for providing fluorogenic label **1**, and G. A. Ellis, J. E. Lomax, and T. Hoang for contributive discussions and critical reading of the manuscript.

## Abbreviations used

<b>CD</b>	cytochalasin D
<b>CPP</b>	cell-penetrating peptide
<b>CPZ</b>	chlorpromazine
<b>CTB</b>	cholera toxin subunit B
<b>ECP</b>	eosinophil cationic protein

<b>EIPA</b>	5-( <i>N</i> -ethyl- <i>N</i> -isopropyl)amiloride
<b>FAM</b>	5- (and 6-) carboxyfluorescein
<b>HSPG</b>	heparan sulfate proteoglycan
<b>M<math>\beta</math>CD</b>	methyl- $\beta$ -cyclodextrin
<b>ONC</b>	Onconase <sup>®</sup> (a registered trademark of Tamir Biotechnology, Inc.; otherwise, ranpirnase)
<b>R<sub>9</sub></b>	nonaarginine
<b>RNase A</b>	bovine pancreatic ribonuclease
<b>TAMRA</b>	5- (and 6-) carboxytetramethylrhodamine
<b>TAT</b>	residues 47–57 of the HIV-1 trans-activator of transcription

## References

1. Fett JW, Strydom DJ, Lobb RR, Alderman EM, Bethune JL, Riordan JF, Vallee BL. Isolation and characterization of angiogenin, an angiogenic protein from human carcinoma cells. *Biochemistry*. 1985; 24:5480–5486. [PubMed: 4074709]
2. Riordan, JF. Structure and function of angiogenin. In: D'Alessio, G.; Riordan, JF., editors. *Ribonucleases: Structures and Functions*. Academic Press; New York: 1997. p. 445-489.
3. Ackerman SJ, Loegering DA, Venge P, Olsson I, Harley JB, Fauci AS, Gleich GJ. Distinctive cationic proteins of the human eosinophil granule: Major basic protein, eosinophil cationic protein, and eosinophil-derived neurotoxin. *J Immunol*. 1983; 131:2977–2982. [PubMed: 6644025]
4. Domachowske JB, Rosenberg HF. Eosinophils inhibit retroviral transduction of human target cells by a ribonuclease-dependent mechanism. *J Leukocyte Biol*. 1997; 62:363–368. [PubMed: 9307075]
5. Johnson RJ, McCoy JG, Bingman CA, Phillips GN Jr, Raines RT. Inhibition of human pancreatic ribonuclease by the human ribonuclease inhibitor protein. *J Mol Biol*. 2007; 367:434–449. [PubMed: 17350650]
6. Lee JE, Raines RT. Ribonucleases as novel chemotherapeutics: The ranpirnase example. *BioDrugs*. 2008; 22:53–58. [PubMed: 18215091]
7. Arnold U. Aspects of the cytotoxic action of ribonucleases. *Curr Pharm Biotechnol*. 2008; 9:1615–1622.
8. Leich F, Stohr N, Rietz A, Ulbrich-Hofmann R, Arnold U. Endocytotic internalization as a crucial factor for the cytotoxicity of ribonucleases. *J Biol Chem*. 2007; 282:27640–27646. [PubMed: 17635931]
9. Benito A, Vilanova M, Ribó M. Intracellular routing of cytotoxic pancreatic-type ribonucleases. *Curr Pharm Biotechnol*. 2008; 9:169–179. [PubMed: 18673282]
10. Conner SD, Schmid SL. Regulated portals of entry into the cell. *Nature*. 2003; 422:37–44. [PubMed: 12621426]
11. Mukherjee S, Ghosh RN, Maxfield FR. Endocytosis. *Physiol Rev*. 1997; 77:759–803. [PubMed: 9234965]
12. Parton RG, Simons K. The multiple faces of caveolae. *Nat Rev Mol Cell Biol*. 2007; 8:185–194. [PubMed: 17318224]
13. Lajoie P, Nabi IR. Regulation of raft-dependent endocytosis. *J Cell Mol Med*. 2007; 11:644–653. [PubMed: 17760830]
14. Cao H, Chen J, Awoniyi M, Henley JR, McNiven MA. Dynamin 2 mediates fluid-phase micropinocytosis in epithelial cells. *J Cell Sci*. 2007; 120:4167–4177. [PubMed: 18003703]
15. Nakase I, Niwa M, Takeuchi T, Sonomura K, Kawabata N, Koike Y, Takehashi M, Tanaka S, Ueda K, Simpson JC, Jones AT, Sugiura Y, Futaki S. Cellular uptake of arginine-rich peptides: Roles for macropinocytosis and actin rearrangement. *Mol Ther*. 2004; 10:1011–1022. [PubMed: 15564133]

16. Jones AT. Macropinocytosis: Searching for an endocytic identity and role in the uptake of cell penetrating peptides. *J Cell Mol Med.* 2007; 11:670–684. [PubMed: 17760832]
17. Doherty GJ, McMahon HT. Mechanisms of endocytosis. *Annu Rev Biochem.* 2009; 78:857–902. [PubMed: 19317650]
18. Rodriguez M, Torrent G, Bosch M, Rayne F, Dubremetz J-F, Ribó M, Benito A, Vilanova M, Beaumelle B. Intracellular pathway of onconase that enables its delivery to the cytosol. *J Cell Sci.* 2007; 120:1405–1411. [PubMed: 17374640]
19. Wu Y, Mikulski SM, Ardelt W, Rybak SM, Youle RJ. A cytotoxic ribonuclease. Study of the mechanism of onconase cytotoxicity. *J Biol Chem.* 1993; 268:10686–10693. [PubMed: 8486718]
20. Haigis MC, Raines RT. Secretory ribonucleases are internalized by a dynamin-independent endocytic pathway. *J Cell Sci.* 2003; 116:313–324. [PubMed: 12482917]
21. Fuchs SM, Rutkoski TJ, Kung VM, Groeschl RT, Raines RT. Increasing the potency of a cytotoxin with an arginine graft. *Protein Eng Des Select.* 2007; 20:505–509.
22. Johnson RJ, Chao T-Y, Lavis LD, Raines RT. Cytotoxic ribonucleases: The dichotomy of Coulombic forces. *Biochemistry.* 2007; 46:10308–10316. [PubMed: 17705507]
23. Turcotte RF, Lavis L, Raines RT. Onconase cytotoxicity relies on the distribution of its positive charge. *FEBS J.* 2009; 276:3846–3857. [PubMed: 19523116]
24. Fan TC, Chang HT, Chen IW, Wang HY, Chang MDT. A heparan sulfate-facilitated and raft-dependent macropinocytosis of eosinophil cationic protein. *Traffic.* 2007; 8:1778–1795. [PubMed: 17944807]
25. Chao T-Y, Lavis LD, Raines RT. Cellular uptake of ribonuclease A relies on anionic glycans. *Biochemistry.* 2010; 49:10666–10673. [PubMed: 21062061]
26. Leland PA, Schultz LW, Kim BM, Raines RT. Ribonuclease A variants with potent cytotoxic activity. *Proc Natl Acad Sci USA.* 1998; 95:10407–10412. [PubMed: 9724716]
27. Lavis LD, Chao TY, Raines RT. Fluorogenic label for biomolecular imaging. *ACS Chem Biol.* 2006; 1:252–260. [PubMed: 17163679]
28. Macia E, Ehrlich M, Massol R, Boucrot E, Brunner C, Kirchhausen T. Dynasore, a cell-permeable inhibitor of dynamin. *Dev Cell.* 2006; 10:839–850. [PubMed: 16740485]
29. Ivanov AI. Pharmacological inhibition of endocytic pathways: Is it specific enough to be useful? *Methods Mol Biol.* 2008; 440:15–33. [PubMed: 18369934]
30. van der Blik AM, Redelmeier TE, Damke H, Tisdale EJ, Meyerowitz EM, Schmid SL. Mutations in human dynamin block an intermediate stage in coated vesicle formation. *J Cell Biol.* 1993; 122:553–563. [PubMed: 8101525]
31. Bayer N, Schober D, Huttinger M, Blaas D, Fuchs R. Inhibition of clathrin-dependent endocytosis has multiple effects on human rhinovirus serotype 2 cell entry. *J Biol Chem.* 2001; 276:3952–3962. [PubMed: 11073943]
32. Subtil A, Hemar A, Dautryvarsat A. Rapid endocytosis of interleukin-2 receptors when clathrin-coated pit endocytosis is inhibited. *J Cell Sci.* 1994; 107:3461–3468. [PubMed: 7706397]
33. Duchardt F, Fotin-Mleczek M, Schwarz H, Fischer R, Brock R. A comprehensive model for the cellular uptake of cationic cell-penetrating peptides. *Traffic.* 2007; 8:849–866.
34. Kirkham M, Parton RG. Clathrin-independent endocytosis: New insights into caveolae and non-caveolar lipid raft carriers. *Biochim Biophys Acta.* 2005; 1745:273–286. [PubMed: 16046009]
35. Dharmawardhane S, Schurmann A, Sells MA, Chernoff J, Schmid SL, Bokoch GM. Regulation of macropinocytosis by p21-activated kinase-1. *Mol Biol Cell.* 2000; 11:3341–3352. [PubMed: 11029040]
36. Kaksonen M, Toret CP, Drubin DG. Harnessing actin dynamics for clathrin-mediated endocytosis. *Nat Rev Mol Cell Biol.* 2006; 7:404–414. [PubMed: 16723976]
37. Fretz M, Jin J, Conibere R, Penning NA, Al-Taei S, Storm G, Futaki S, Takeuchi T, Nakase I, Jones AT. Effects of Na<sup>+</sup>/H<sup>+</sup> exchanger inhibitors on subcellular localisation of endocytic organelles and intracellular dynamics of protein transduction domains HIV-TAT peptide and octarginine. *J Control Release.* 2006; 116:247–254. [PubMed: 16971016]

38. Patki V, Virbasius J, Lane WS, Toh BH, Shpetner HS, Corvera S. Identification of an early endosomal protein regulated by phosphatidylinositol 3-kinase. *Proc Natl Acad Sci USA*. 1997; 94:7326–7330. [PubMed: 9207090]
39. Kjekken R, Mousavi SA, Brech A, Griffiths G, Berg T. Wortmanin- sensitive trafficking steps in the endocytic pathway in rat liver endothelial cells. *Biochem J*. 2001; 357:497–503. [PubMed: 11439100]
40. Ullrich O, Reinsch S, Urbe S, Zerial M, Parton RG. Rab11 regulates recycling through the pericentriolar recycling endosome. *J Cell Biol*. 1996; 135:913–924. [PubMed: 8922376]
41. Torgersen ML, Skretting G, van Deurs B, Sandvig K. Internalization of cholera toxin by different endocytic mechanisms. *J Cell Sci*. 2001; 114:3737–3747. [PubMed: 11707525]
42. Langel, Ü., editor. *Handbook of Cell-Penetrating Peptides*. 2. CRC Press; Boca Raton, FL: 2007.
43. Wadia JS, Stan RV, Dowdy SF. Transducible TAT-HA fusogenic peptide enhances escape of TAT-fusion proteins after lipid raft macropinocytosis. *Nat Med*. 2004; 10:310–315. [PubMed: 14770178]
44. Richard JP, Melikov K, Brooks H, Prevot P, Lebleu B, Chernomordik LV. Cellular uptake of unconjugated TAT peptide involves clathrin-dependent endocytosis and heparan sulfate receptors. *J Biol Chem*. 2005; 280:15300–15306. [PubMed: 15687490]
45. Zhang XP, Jin YJ, Pllummer MR, Pooyan S, Gunaseelan S, Sinko PJ. Endocytosis and membrane potential are required for HeLa cell uptake of R.I.-CKTat9, a retro-inverso Tat cell penetrating peptide. *Mol Pharm*. 2009; 6:836–848. [PubMed: 19278221]
46. Fuchs SM, Raines RT. Pathway for polyarginine entry into mammalian cells. *Biochemistry*. 2004; 43:2438–2444. [PubMed: 14992581]
47. Lavis LD, Rutkoski TJ, Raines RT. Tuning the  $pK_a$  of fluorescein to optimize binding assays. *Anal Chem*. 2007; 79:6775–6782. [PubMed: 17672523]
48. Skretting G, Torgersen ML, van Deurs B, Sandvig K. Endocytic mechanisms responsible for uptake of GPI-linked diphtheria toxin receptor. *J Cell Sci*. 1999; 112:3899–3909. [PubMed: 10547351]
49. Rutkoski TJ, Kurten EL, Mitchell JC, Raines RT. Disruption of shape-complementarity markers to create cytotoxic variants of ribonuclease A. *J Mol Biol*. 2005; 354:41–54. [PubMed: 16188273]
50. Gitay-Goren H, Soker S, Vlodavsky I, Neufeld G. The binding of vascular endothelial growth-factor to its receptors is dependent on cell surface-associated heparin-like molecules. *J Biol Chem*. 1992; 267:6093–6098. [PubMed: 1556117]
51. Rapraeger AC, Guimond S, Krufka A, Olwin BB. Regulation by heparan-sulfate in fibroblast growth-factor signaling. *Methods Enzymol*. 1994; 245:219–240. [PubMed: 7760735]
52. Tkachenko E, Lutgens E, Stan RV, Simons M. Fibroblast growth factor 2 endocytosis in endothelial cells proceed via syndecan-4 dependent activation of Rac1 and a Cdc42-dependent macropinocytic pathway. *J Cell Sci*. 2004; 117:3189–3199. [PubMed: 15226395]
53. Lampugnani MG, Orsenigo F, Gagliani MC, Tacchetti C, Dejana E. Vascular endothelial cadherin controls VEGFR-2 internalization and signaling from intracellular compartments. *J Cell Biol*. 2006; 174:593–604. [PubMed: 16893970]
54. Patel LN, Zaro JL, Shen WC. Cell penetrating peptides: Intracellular pathways and pharmaceutical perspectives. *Pharm Res*. 2007; 24:1977–1992. [PubMed: 17443399]
55. Futaki S, Nakase I, Taclokoro A, Takeuchi T, Jones AT. Arginine-rich peptides and their internalization mechanisms. *Biochem Soc Trans*. 2007; 35:784–787. [PubMed: 17635148]
56. Noguchi H, Bonner-Weir S, Wei FY, Matsushita M, Matsumoto S. BETA2/NeuroD protein can be transduced into cells due to an arginine- and lysine-rich sequence. *Diabetes*. 2005; 54:2859–2866. [PubMed: 16186386]
57. Kerkis A, Kerkis I, Radis-Baptista G, Oliveira EB, Vianna-Morgante AM, Pereira LV, Yamane T. Crotonamine is a novel cell-penetrating protein from the venom of rattlesnake *Crotalus durissus terrificus*. *FASEB J*. 2004; 18:1407–1409. [PubMed: 15231729]
58. Klink TA, Raines RT. Conformational stability is a determinant of ribonuclease A cytotoxicity. *J Biol Chem*. 2000; 275:17463–17467. [PubMed: 10747991]
59. Rutkoski TJ, Raines RT. Evasion of ribonuclease inhibitor as a determinant of ribonuclease cytotoxicity. *Curr Pharm Biotechnol*. 2008; 9:185–199. [PubMed: 18673284]

60. Fuchs SM, Raines RT. Arginine grafting to endow cell permeability. *ACS Chem Biol.* 2007; 2:167–170. [PubMed: 17319644]
61. Cronican JJ, Thompson DB, Beier KT, McNaughton BR, Cepko CL, Liu DR. Potent delivery of functional proteins into mammalian cells in vitro and in vivo using a supercharged protein. *ACS Chem Biol.* 2010; 5:747–752. [PubMed: 20545362]



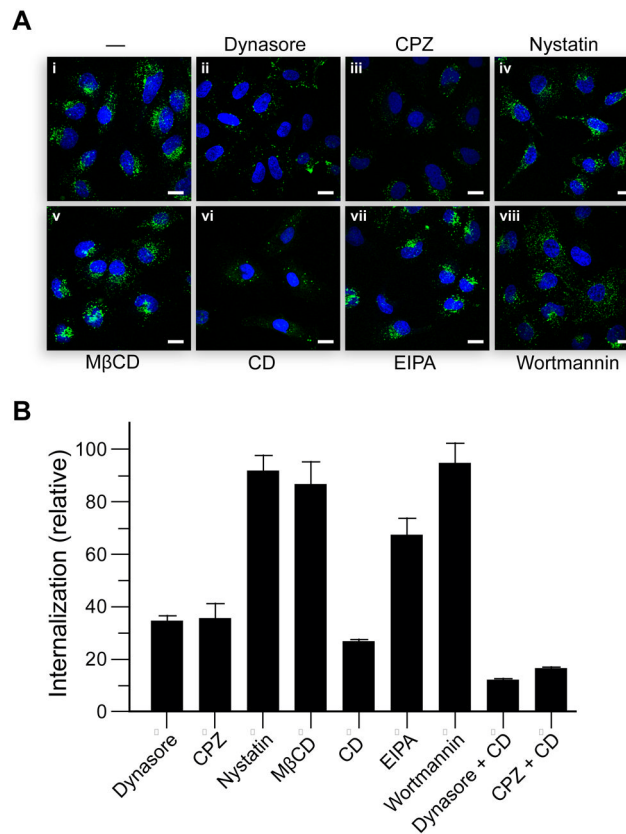


**Figure 1.**

Effect of endocytic inhibitors on RNase A-uptake. HeLa cells at 37 °C were pretreated with endocytic inhibitors for 30 min, and then incubated with fluorogenic RNase A for 1 h in the presence of the inhibitors. (A) Confocal microscopy. (i) Untreated cells; (ii) dynasore at 80  $\mu$ M; (iii) CPZ at 10  $\mu$ g/mL; (iv) nystatin at 25  $\mu$ g/mL; (v) M $\beta$ CD at 5 mM; (vi) CD at 5  $\mu$ g/mL; (vii) EIPA at 10  $\mu$ M; (viii) wortmannin at 50 nM. Scale bars: 10  $\mu$ m. (B) Flow cytometry. Data are mean values ( $\pm$ SE) of total fluorescence for 20,000 washed cells from  $\geq$ 6 cell populations.

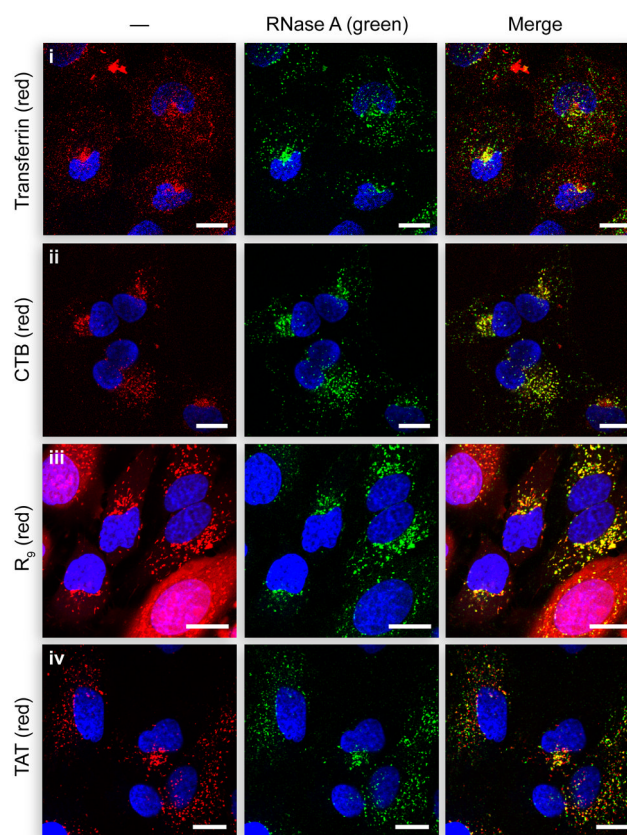


**Figure 2.** Colocalization of RNase A with endocytic markers. Confocal microscopy of HeLa cells incubated with fluorogenic RNase A (27) (10  $\mu$ M) and (i) Alexa Fluor 594–transferrin (1  $\mu$ M), (ii) Alexa Fluor 594–CTB (1  $\mu$ g/mL), (iii) 10  $\mu$ M TAMRA–R<sub>9</sub> (10  $\mu$ M), or (iv) TAMRA–TAT (10  $\mu$ M) for 1 h at 37 °C, and washed. Incubations with CPPs followed a 15-min pretreatment with RNase A. Scale bars: 10  $\mu$ m.

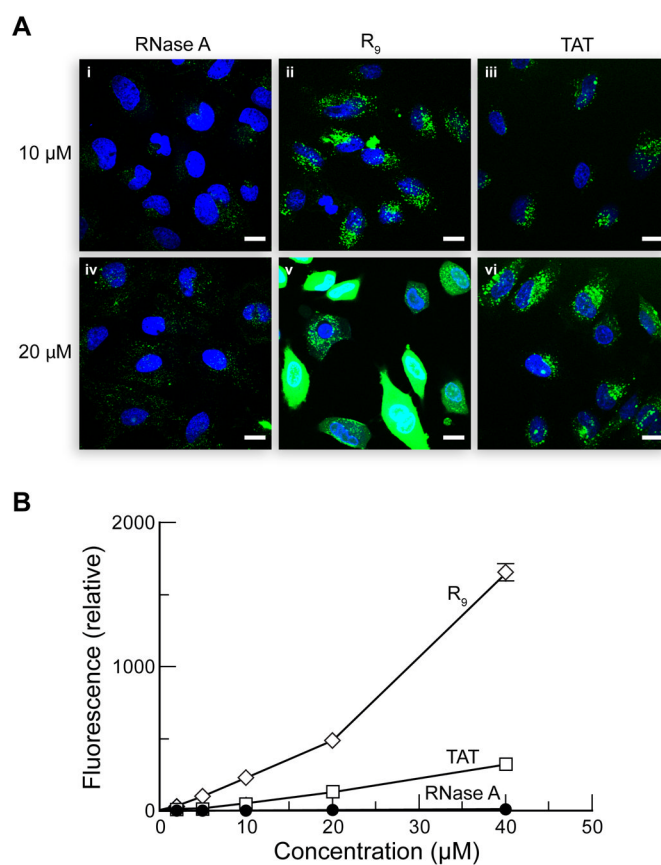


**Figure 3.** Concentration-dependence of RNase A- and CPP-uptake. (A) Confocal microscopy. HeLa cells were incubated with fluorescein–RNase A (i and iv), FAM– $R_9$  (ii and v), and FAM–TAT (iii and vi) for 1 h at 37 °C, and washed. Scale bars: 10  $\mu\text{m}$ . (B) Flow cytometry. Data points are mean values ( $\pm\text{SE}$ ) of total fluorescence for 20,000 washed cells from 3 cell populations.

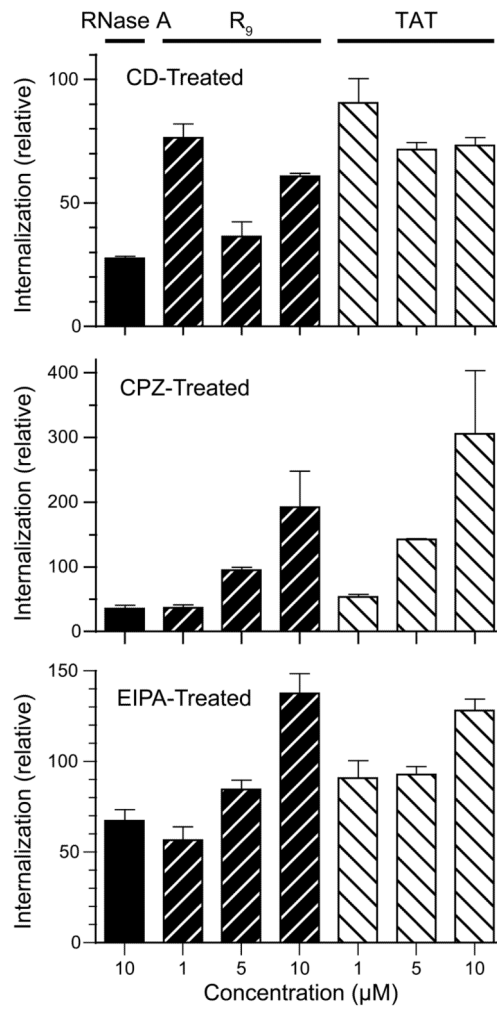


**Figure 4.** Comparative effect of endocytic inhibitors on RNase A- and CPP-uptake HeLa cells at 37 °C were pretreated with CD, CPZ, or EIPA for 30 min, and then incubated with fluorogenic RNase A, FAM-R<sub>9</sub>, or FAM-TAT for 1 h in the presence of the endocytic inhibitors. Data are mean values ( $\pm$ SE) of total fluorescence for 20,000 washed cells from  $\geq 6$  cell populations.

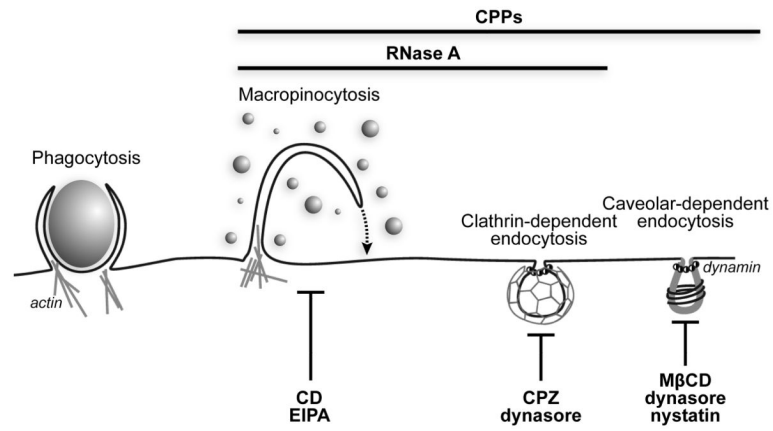


**Figure 5.** Portals of entry into a mammalian cell. RNase A and CPPs enter cells in a similar manner as discerned, in part, by the blocking of portals with the indicated drugs. Image was adapted from ref. 10.



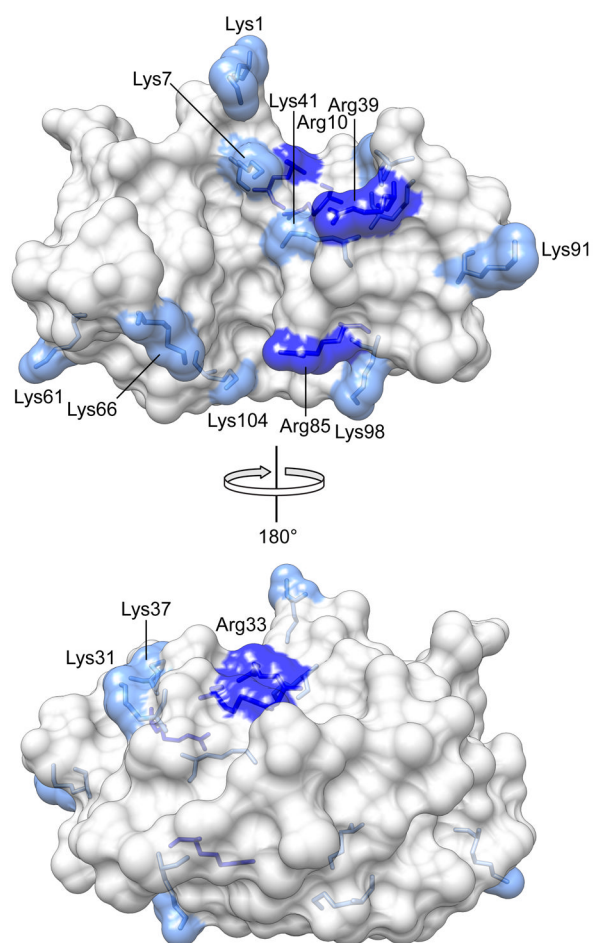


**Figure 6.** Cationic residues of RNase A. Lysine residues (10) are light blue; arginine residues (4) are dark blue. A large cationic patch consists of Lys1, Lys7, Arg10, Lys37, Arg39, and Lys41. A small cationic patch consists of Lys66, Arg85, Lys98, and Lys104.

**Table 1**

## Protein Transduction Properties of RNase A and CPPs

	<b>RNase A</b>	<b>R<sub>9</sub></b>	<b>TAT</b>
Total residues	124	9	11
Arginine residues	4	9	6
Lysine residues	10	0	2
Net charge	+4	+9	+8
Cell-surface receptors	Heparan sulfate proteoglycans Chondroitin sulfate proteoglycans Sialic acid-containing glycoproteins	Heparan sulfate proteoglycans Chondroitin sulfate proteoglycans	
Cell-types targeted	All cell types	All cell types	
Mechanism of internalization	Clathrin-mediated endocytosis Macropinocytosis	Clathrin-mediated endocytosis Caveolar-mediated endocytosis Macropinocytosis Possible non-endocytic mechanism	